The Effect of Artificial Surface Roughness on Heat and Momentum Transfer

D. W. SAVAGE and J. E. MYERS

Purdue University, Lafayette, Indiana

Heat transfer from rough surfaces to flowing fluids is of interest because of the high heat transfer rates that can be obtained in equipment of small volume. The increase in heat transfer rate is generally owing to both an increase in the area of the surface and an increase in the heat transfer coefficient. The increase in heat transfer coefficient is owing to a change in the turbulence pattern close to the wall brought about by the presence of the surface protuberances. Unfortunately, the increase in heat transfer rate brought about by roughening a surface is usually accompanied by a large increase in the energy needed to move the fluid across the surface; as a consequence the heat transfer per unit of power consumption is often less for a rough surface than for a smooth surface. It is therefore of economic, as well as academic, interest to determine what type or types of roughness will produce the maximum rate of heat transfer per unit of power consumption.

The approach adopted in this study was to consider a simple type of roughened surface, transverse fins on the inside wall of a circular pipe, and focus attention on one single test fin. Arrays of identical fins were placed upstream and downstream from the test fin to establish a developed velocity field at the test fin and to provide a roughened length over which overall pressure-drop measurements could be taken. The actual experimental system employed had a test fin, at which heat transfer and form drag measurements were made, that was integral with the pipe wall. The arrays of fins on either side of the test fin were a sliding fit in the circular pipe making it relatively easy to vary the spacing between consecutive fins.

The main objectives of the research were to measure the contribution of form drag to the total forces retarding flow for different roughness configurations and Reynolds numbers, and to measure the average heat transfer coefficient around a typical single protuberance as well as the effect of fin height and fin spacing on this average coefficient. The effect of Prandtl number was also studied.

THEORY AND PREVIOUS WORK

Past work can be classified in terms of the flow regime in which the studies were made. The term "transition regime" refers to flow and roughness conditions for which the overall friction coefficient depends on both the roughness and the Reynolds number. The term "fully rough regime" describes conditions where the overall friction coefficient is independent of Reynolds number and depends only on the roughness.

The effect of wall roughness in conduits on heat and momentum transfer has been studied by many workers. Early friction studies were made by Nikuradse (*1*) and Schlichting (*2*); heat and momentum transfer studies in the transition flow regime have been made by Stanton (*3*), Kemeny and Cyphers (*4*), Smith and Epstein (*5*), and Hastrup et al. (*6*). For the fully rough flow region, which is the flow condition which prevailed in the experiments described here, the literature contains reports of investigations by Cope (*7*), Dipprey (*8*), Boelter et al. (*9*), Sams (*10*), Brouillette et al. (*11*), Nunner (*12*), and Koch (*13*). Both Knudsen and Katz (*14*) and Atherton and Thring (*18*) have studied fully rough flow in an annulus having transverse fins on the outer surface of the inner tube. The results obtained by Cope and Dipprey are not strictly comparable with those of the present investigation as they did not use a transverse-fin type of surface.

Boelter et al. used a system consisting of two parallel flat plates with thin strips of metal soldered to one of the plates normal to the direction of air flow. Heat transfer was improved 50 to 200% by the addition of the fins, but increasing the fin height above one eighth of the channel width gave little improvement in heat transfer and increased the pressure drop considerably. Brouillette et al. studied the pressure drop and heat transfer characteristics of water flowing through copper tubes with internal fins produced by cutting 60 deg. V-shaped notches in the inner surface. Friction factors for rough tubes were greater than smooth-tube values by amounts varying from 15 to 400%. In comparison, heat transfer coefficients were only 15 to 100% greater than smooth-tube values. Both notch height and number of notches per inch affected the friction factors whereas for heat transfer the effect of height was much greater than that of spacing.

Nunner carried out an extensive series of measurements using circular tubes roughened by means of uniformly spaced piston rings. The Nusselt numbers calculated by Nunner increased with roughness up to 2.8 times the

D. W. Savage is with the Atomic Energy Research Establishment, United Kingdom Atomic Energy Authority, Harwell, Berkshire, England.

smooth values. With the assumption that roughness acts only to reduce the resistance of the turbulent core, the resistance at the wall being the same as in a smooth tube, Nunner modified the Prandtl-Taylor equation to obtain the relationship

$$N_{St} = \frac{f_r/2}{1 + 1.5\,(N_{Re})^{-1/8}\,(N_{Pr})^{-1/6}\,[(N_{Pr})\,(f_r/f_o) - 1]}$$

The grouping in the denominator $(N_{Pr})\,(f_r/f_o)$ reflects the proposal, which has some experimental support from Nunner's temperature profiles, that increasing the roughness in a rough tube has an effect similar to that of increasing the Prandtl number. Koch extended Nunner's experiments to large roughness heights and spacings. He found that for small roughness heights (up to about $e/D = 0.03$) the ratios $(N_{Nu})_r/(N_{Nu})_o$ and f_r/f_o increase almost in direct proportion to one another. A further increase in heat transfer obtained using larger fin heights is obtained at the expense of a large increase in friction coefficient. For a given roughness height, the effect of roughness spacing, in the range $4 < L/e < 20$, on the Nusselt number was found to be quite small.

Knudsen and Katz, with water flowing in an annular passage containing circular fins on the inside wall of the annulus, showed the existence of different types of well-defined eddies between the fins by injecting colored dye into the water. For $e/L = 1.0$ there was one single eddy which almost filled the fin space, and for $e/L = 2.0$ there were two counter rotating eddies, one above the other. The annulus investigated by Atherton and Thring had very small fin spacing, in the range $1.65 < e/L < 5.8$. In this range, the overall friction coefficients increased as the fin spacing decreased. For constant height and spacing, the friction coefficient decreased with increasing fin width.

Wilson (*15*) measured the velocity field between consecutive fins in a large-scale, two-dimensional model of a circumferentially finned can. His results showed that even for spacings that were small relative to the fin height $(e/L = 2.6)$, there was circulatory motion extending down to the base wall. Harris and Wilson (*16*) showed that the variation of heat transfer coefficient around the fin sides was that which might be expected from the presence of well-defined eddies between the fins.

The total drag on a transversely finned surface will be the algebraic sum of the form drag of each fin and the skin friction forces at the base wall between fins and at the fin tips. There will also be skin friction forces acting on the sides of the fins in a direction normal to that of the main flow. Form drag is owing to the unsymmetrical pressure distribution around the fins; skin friction is the shear stress at the surface owing to velocity gradients in the boundary layers. The analysis carried out in this study, based on an overall momentum balance in the direction of the pipe axis, provides no information on the skin frictional force acting in the radial direction. The radial skin frictional forces will depend on the velocity of circulation of the eddies between the fins, the rotation of the eddies being maintained by momentum exchange with the main stream.

TABLE 1. RANGE OF EXPERIMENTAL CONDITIONS INVESTIGATED

Empty diameter of test section, $D = 6.065$ in.
Fin height $= e$
Fin spacing $= L$
Reynolds number range, $10^4 < N_{Re\,D} < 1.3 \times 10^5$
Prandtl number range, $2.8 < N_{Pr} < 8.0$
Fluid—demineralized water

Roughness configuration	Fin height e (in.)	Fin spacing L (in.)
1	1	1.0
2	1	2.0
3	1	3.0
4	1	5.0
5	1	8.0
6	1	13.0
7	1	∞
8	0.75	0.5
9	0.75	1.0
10	0.75	3.0
11	0.75	5.0
12	0.75	8.0
13	0.75	∞
14	0.5	0.5
15	0.5	1.0
16	0.5	3.0
17	0.5	8.0
18	0.5	∞
19	0.25	0.5
20	0.25	1.0
21	0.25	2.0
22	0.25	3.0
23	0.25	∞
24	0	

EXPERIMENTAL WORK

The experiments were carried out with circular tubes containing protuberances on the inside wall. A roughened length with protuberances that were fitted tightly, but were not integral with the wall, was used to establish the flow pattern and measure overall pressure drop. These protuberances were

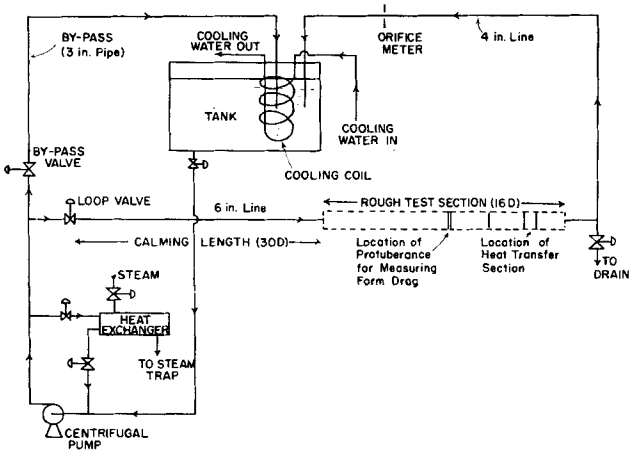

Fig. 1. General arrangement of experimental equipment.

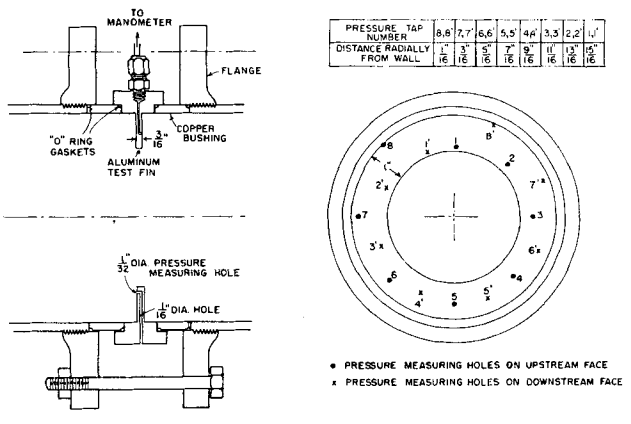

Fig. 2. Detailed diagram of special protuberance for measuring form drag.

formed by spacing annular disks, each 0.088-in. thick, uniformly inside a smooth circular pipe at right angles to the pipe axis. Each roughness element was therefore an internal transverse circular fin. Special protuberances, each 3/16-in. thick, integral with the wall, were included in the region of developed flow to make heat transfer and form drag measurements.

The test sections and the smooth upstream and downstream sections were constructed from steel pipe having an internal diameter of 6.065 in. Fin heights and fin spacings used are given in Table 1, and the arrangement of the experimental apparatus is shown in Figure 1.

The total loss in energy experienced by the water flowing through the rough test section, which included both skin friction and form drag, was measured by means of static-pressure tubes located at the pipe center line. The distance between the measuring stations was about 5 ft.

The concept of developed flow, in the sense used to describe developed flow in a smooth pipe, does not exist with this type of roughness. A certain distance downstream from the beginning of the roughened length, however, the flow will be developed in the sense that the flow pattern is repeated identically between each pair of consecutive roughness elements. If the static-pressure measuring holes are the same distance behind the nearest roughness element, the true static pressure drop will be obtained. This condition was closely approximated for all roughness spacings except the spacing $L = 13$ in. For this case a small correction was made on the basis of the measured pressure gradient along the wall between two roughness elements.

Form drag was determined from pressure measurements on the single fin shown in Figure 2. Sixteen pressure taps were used when the fin was 1 in. high. As the fin was cut to lower heights some of the original taps were lost until, for the 0.25-in. high fin, only four remained. Differential pressure readings were observed on a micromanometer.

The attainment of a developed temperature profile in a liquid flowing in a 6-in. pipe is difficult experimentally because of the large energy requirement and was never attempted. This investigation was primarily concerned with the relative effect on heat transfer of the different parameters characterizing surface geometry and not with absolute magnitudes. Hence it was decided to heat only a short length of pipe wall containing a typical protuberance integral with the wall, and determine the effect of Reynolds number, Prandtl number, fin height, and fin spacing on the average heat transfer coefficient of this heated element.

Figure 3 shows the single fin used for the heat transfer measurements. With the 1.0-in. high fin there were twenty thermocouples embedded in the finned section as shown in Figure 4. Pairs of thermocouples in each given radial-axial position were separated by at least 90 deg. to test for possible angular temperature variations. All thermocouples were made from number 30 copper-constantan wire.

For heat transfer runs at low fin heights, some of the thermocouple sites were removed when the fin was machined down. The final runs were made with the fin completely machined off the test section to produce a smooth tube thermal entrance section.

ANALYSIS OF MEASUREMENTS

Calculation of Friction Coefficients

The pressure drop for flow in the rough tube is represented in terms of a friction coefficient f_T which is defined by

$$f_T = \frac{2\, g_c\, \bar{\tau}}{\rho\, \bar{U}^2} \tag{1}$$

where $\bar{\tau}$ is the average resisting stress at the wall made up of both skin friction and form drag, and $\bar{U}$ is the average velocity in the tube and is based on some equivalent diameter. The choice of equivalent diameter affects the magnitude of the friction coefficient considerably, because the friction coefficient depends on the diameter to the fifth power. The results are presented in terms of a friction coefficient based on the minimum diameter of the rough tube which is the diameter level with a roughness element, $D - 2e$. The expression for the overall friction coefficient using this equivalent diameter becomes

$$f_T = \frac{\Delta p_T}{X} \cdot \frac{g_c (D - 2e)}{2\, \rho\, \bar{U}^2_{D-2e}} \tag{2}$$

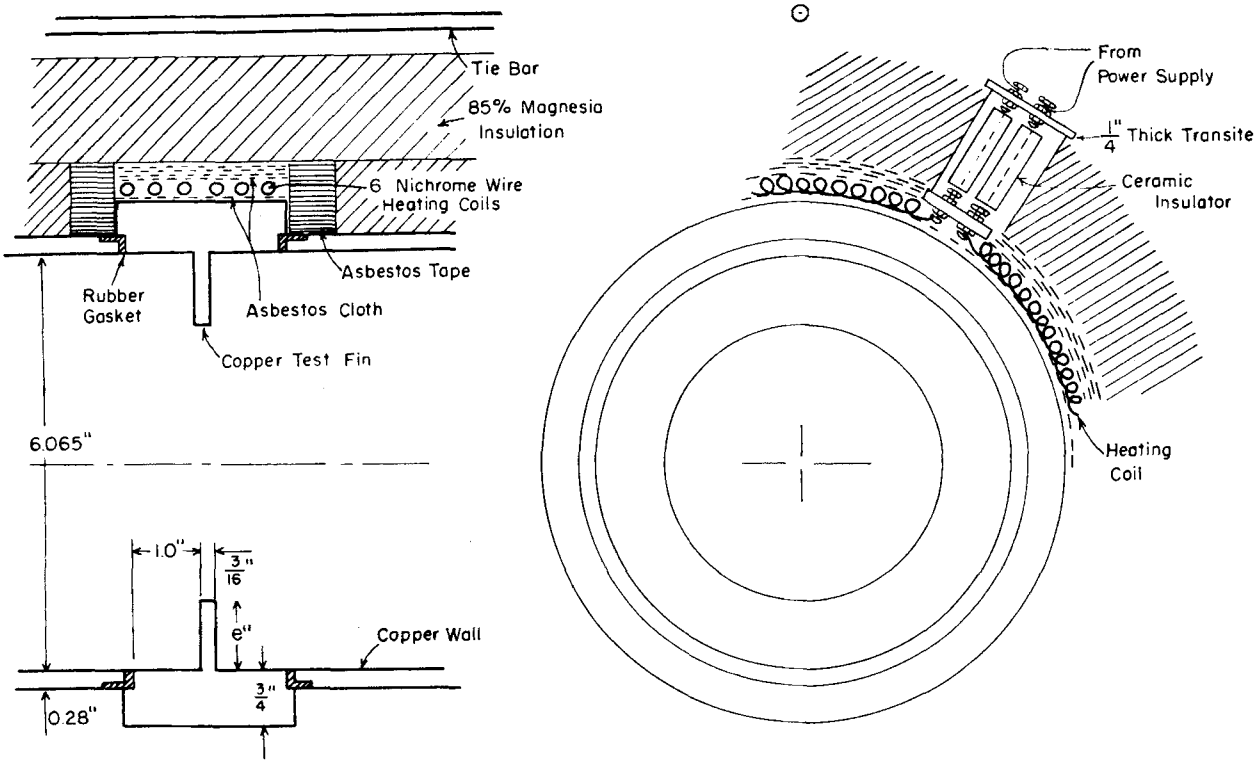

Fig. 3. Detailed diagram of integral fin for making heat transfer measurements.

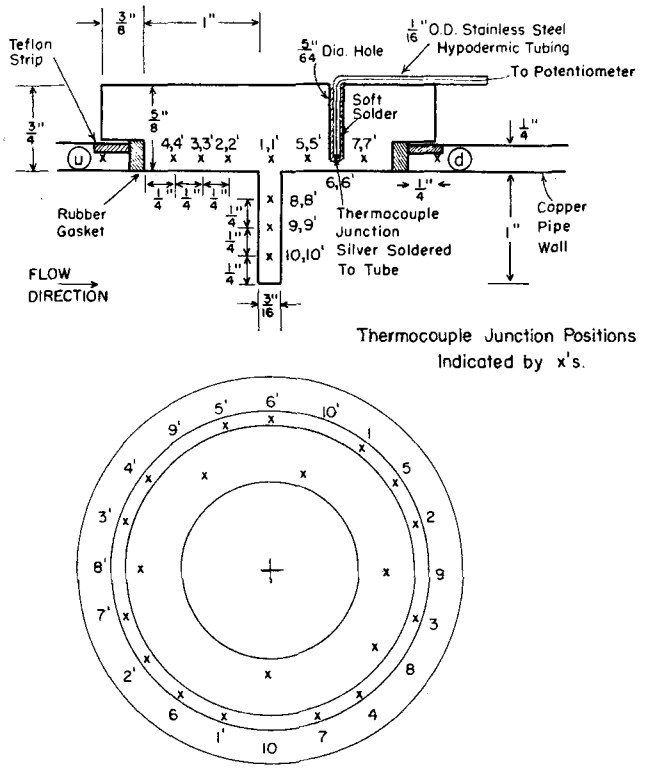

Fig. 4. Positions of thermocouple junctions and method of thermocouple installation.

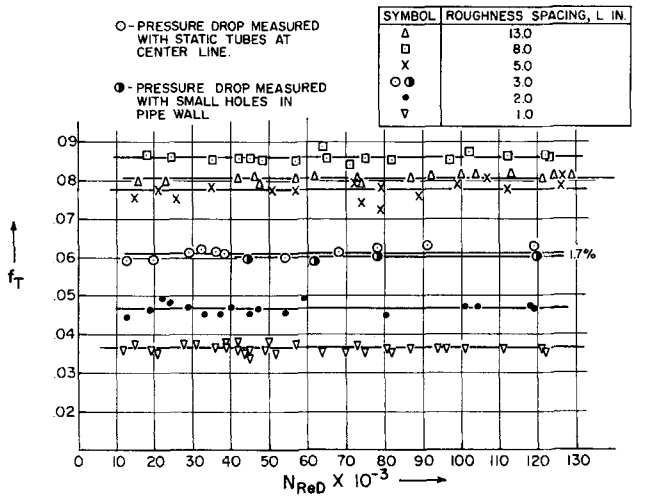

Fig. 5. Dependence of overall friction coefficient on Reynolds number for roughness height, e = 1.0 in.

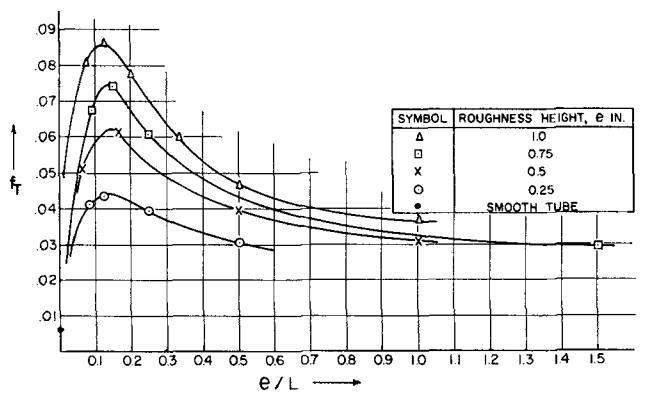

Fig. 6. Dependence of overall friction coefficient on the ratio: roughness height/roughness spacing ($10^4 < N_{Re\,D} < 10^5$).

where Δp_T is the total pressure drop between the measuring points, $\overline{U}_{D-2e} = 4G/(\pi\rho(D-2e)^2)$, and G is the mass rate of flow.

If a force-momentum balance is written on a length of rough pipe one sees that the accelerating force is $(\pi D^2/4)(p_1 - p_2)$. The retarding forces are the total form drag $D_F = n\,D'_F$ where D'_F is the form drag of one roughness element and n is the number of elements, and the net force due to shear stress in the direction of flow $D_{S,x}$. The opposing force terms may be equated and solved for the net skin frictional drag

$$D_{S,x} = \frac{\pi D^2}{4}(p_1 - p_2) - n\,D'_F \tag{3}$$

Form drag is defined as the net normal pressure force, in the direction of flow, acting on the surface of a roughness element. It can be calculated by measuring the pressure distribution around the element and then integrating the pressure over the total area normal to flow. The pressure at position y on the upstream face of a roughness element is designated as p_{yu} and on the downstream face p_{yd}. The net pressure force, form drag, on one roughness element is the algebraic sum of these two forces; that is

$$D'_F = \int\int_{A_s} (p_{yu} - p_{yd})\,dA_s \tag{4}$$

The form drag was evaluated by plotting $(p_{yu} - p_{yd})$ against the normal area A_s (ft.^{2}), and integrating graphically using a planimeter. The form drag coefficient f_F is defined by the equation

$$f_F = \frac{2g_c\,D'_F}{\rho A_s \overline{U}^2_{D-2e}} \tag{5}$$

where A_s is the normal area of one side of a roughness element. The skin friction coefficient is defined by an equation similar to that used in defining the overall friction coefficient

$$fs = \frac{\Delta p_S}{X} \cdot \frac{g_c(D-2e)}{2\,\rho\,\overline{U}^2_{D-2e}} \tag{6}$$

In this expression Δp_S, the pressure drop owing to the skin frictional drag force is equal to $D_{S,x}/(\pi D^2/4)$.

The friction coefficients described above are shown plotted against a Reynolds number defined as

$$N_{Re\,D} = \frac{D\,\overline{U}_D}{\nu} \tag{7}$$

where $\overline{U}_D$ is the bulk velocity based on the empty 6-in. pipe.

Calculation of Heat Transfer Coefficients

The mean heat transfer coefficient for the heated section was calculated from the equation

$$q = h\,A\,(T_w - T_b) \tag{8}$$

The heat transfer rate to the water q is the rate of heat generation in the electric coils minus the rate of heat loss. Some heat was lost by conduction axially from the heated element through the rubber gasket to the adjacent copper wall. This loss was calculated from thermocouple readings in the heated element and in the adjacent wall and was subtracted from the input. The maximum loss by this mechanism was 7%, but for most runs was of the order of 2 to 5%. The other loss was from conduction through the insulation and convection to the surrounding atmosphere. This was found to be uniform at about 3% of the power input and was ignored in calculating the heat transfer coefficients.

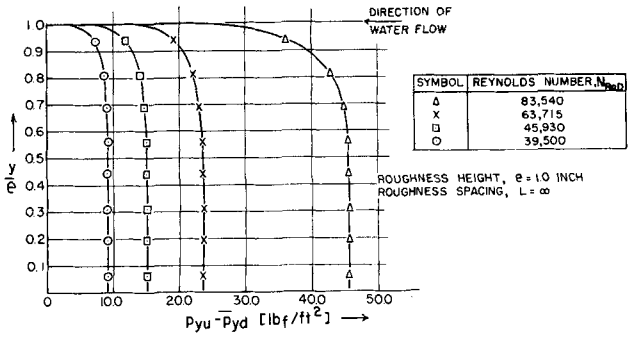

Fig. 7. Pressure distribution around a roughness element for $e/L = 0$.

The area in Equation (8) was taken as the internal area of the heated element. This included the area of the protuberance (which varied with fin height) and the area of the 1-in. wide wall section on each side of the base of the fin. The wall temperature T_w was obtained from the readings on the thermocouples in the fin and wall of the element. The value taken for T_w was the mean of the readings, each weighted according to the surface area represented. The temperature drops between the thermocouple locations and the inner surface of the wall were negligible. The term T_b in Equation (8) was taken as the bulk temperature of the water at the entrance to the short heated section.

Runs were made at different bulk fluid temperatures and with different temperature driving forces so it was necessary to correct the heat transfer coefficients calculated from Equation (8) for radial variation in physical properties. This was done by multiplying h by $(\mu_w/\mu_b)^{0.14}$ as suggested by Sieder and Tate (*17*). The use of this parameter was found to be valid by the results of experiments in which the Reynolds number, bulk fluid Prandtl number, and surface roughness were held constant while the power input was varied.

EXPERIMENTAL RESULTS

Overall Friction Coefficients

The overall friction coefficients were calculated from Equation (2). Sample results are shown in Figure 5 for the experiments with 1-in. fins ($e/D = 0.165$). For this fin height, as well as for the 3/4-, 1/2-, and 1/4-in. fins, the friction coefficients were found to be independent of Reynolds number. The overall friction coefficients for all four fin heights are shown plotted against the relative fin spacing e/L in Figure 6. At very large spacings ($e/L \rightarrow 0$) all curves approach the smooth-tube value. The curve for each fin height passes through a maximum at $e/L \sim 1/9$ and then falls gradually as the fin spacing decreases. At very small spacings ($e/L \rightarrow \infty$) the curves appear to become horizontal, but they must eventually approach the smooth-tube value also. However, this would not be observed until the spacing approached microscopic dimensions. It would seem likely that for $e/L >> 1$ the magnitude of the friction coefficient would depend critically on the shape of the tips of the roughness elements. For spacings in the vicinity of $e/L = 1$, the curves appear to come together being independent of spacing and only slightly dependent on fin height.

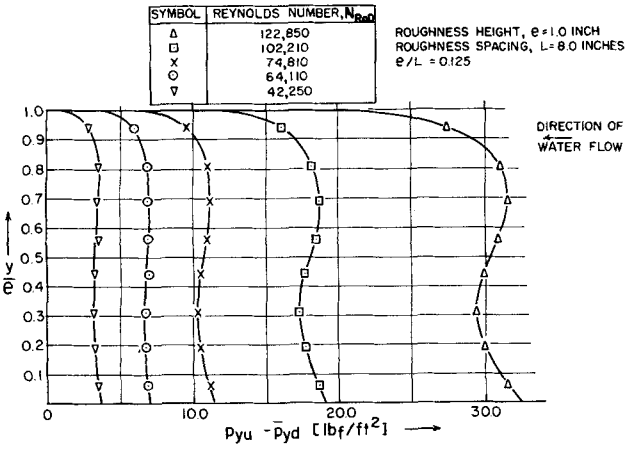

Fig. 8. Pressure distribution around a roughness element for $e/L = 0.125$.

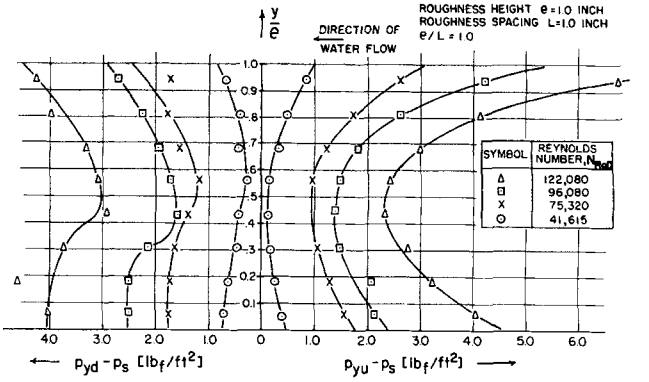

Fig. 9. Pressure distribution around a roughness element for $e/L = 1.0$.

Pressure Distributions

The normal pressure distribution on a fin was measured for fin heights of 1, 0.75, 0.5, and 0.25 in. and for as many as seven spacings for each fin height. Only the results for three spacings using 1-in. fins are shown here, but these indicate the nature of the results obtained for all conditions studied.

Figure 7 shows the pressure distribution for a single fin ($e/L = 0$). For this situation, which is equivalent to that obtained with flow through an orifice meter, the pressure on the downstream face was independent of radial position, and the figure shows the difference between upstream and mean downstream pressures plotted against the dimensionless distance from the base of the fin (y/e). The pressure on the upstream face is constant over the lower part of the fin and falls off steeply as the fin tip is approached.

Figure 8 shows the pressure distribution for a spacing of 8 in. For this arrangement the pressure was also uniform at all taps on the downstream face of the fin for all flow rates. On the upstream face the curves for low flow rates are similar to the curves in Figure 7, though the

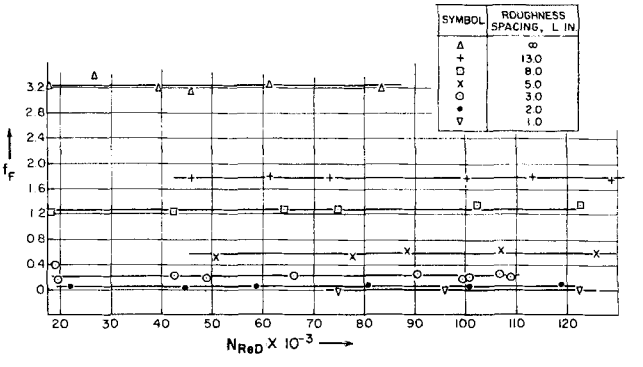

Fig. 10. Dependence of form drag coefficient on Reynolds number for roughness height, $e = 1.0$ in.

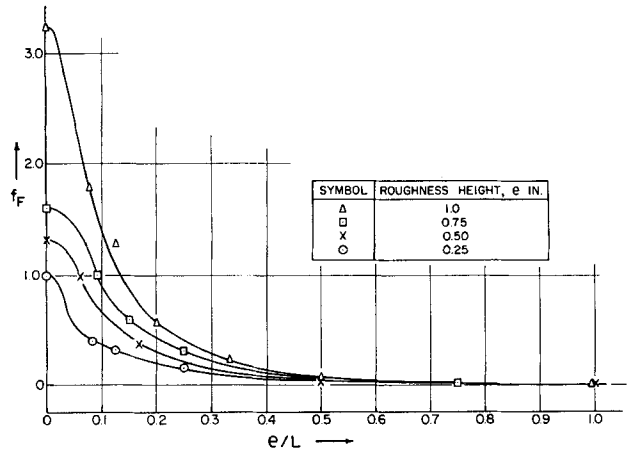

Fig. 11. Dependence of form drag coefficient on the ratio roughness height/roughness spacing ($10^4 < N_{Re\,D} < 10^5$).

net pressures differ substantially when the two systems are compared at the same flow rate. At high flow rates the pressure distribution on the upstream face shows two maxima indicating the presence of a flow disturbance upstream.

This shape of pressure distribution was found on the upstream face of the test fin for the closer spacings of 5, 3 and 2 in., but the magnitudes of the pressures at equivalent flow rates decreased considerably. However, for a spacing of 1 in. ($e/L = 1$), a different pressure distribution was found. In this case the pressure distribution on the downstream face of the test fin was found to be nonuniform at all flow rates. For this reason the pressure distributions are shown for both faces in Figure 9. The common reference pressure p_s referred to in this figure was the static pressure taken from the static pressure side of a Pitot tube placed at the pipe center line level with the test fin. On both upstream and downstream faces the pressure is high near the base wall and near the fin tips and passes through a minimum at $y/e \sim 0.5$. The pressure distributions are not only similar in shape on both sides of the fin, but also similar in magnitude. In fact, integration of the readings over the fin surfaces showed them to be equal, so that the net normal force or form drag was found to be zero.

The results obtained with 0.75- and 0.50-in. fins were similar to those obtained using 1-in. fins. In all cases the form drag decreased from a maximum at $L = \infty$ to zero at $L = e$.

The shapes of the pressure distributions described above support the visual findings of Knudsen and Katz

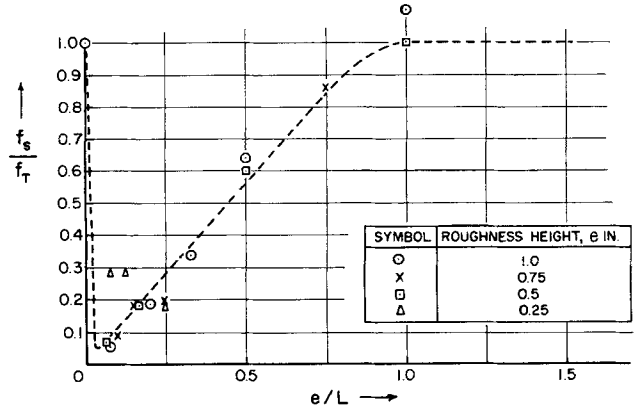

Fig. 12. Contribution of skin friction to the total pressure drop ($N_{Re\,D} = 10^5$).

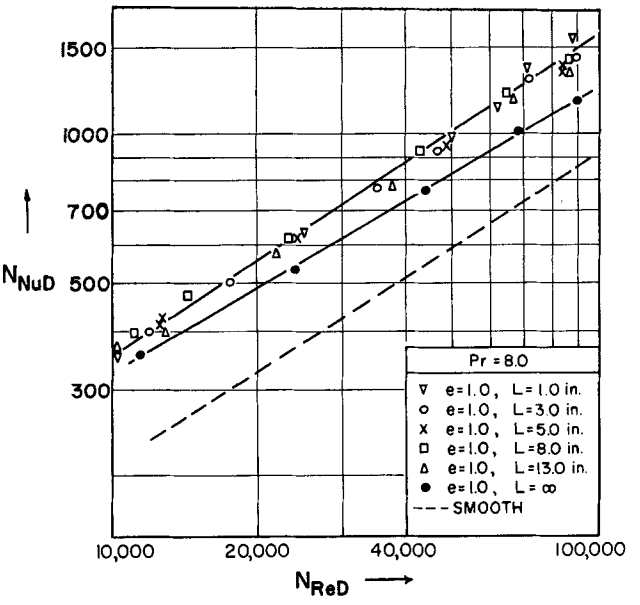

Fig. 13. Dependence of heat transfer coefficient on Reynolds number for e = 1.0 in.

(*14*) that well-defined eddies exist between fins in this type of system. The results indicate that the length of the eddy which forms behind a fin is certainly five fin heights long and may be as much as eight. For most spacings studied the eddy lies slightly downstream from a fin and there is therefore a region, directly behind the fin, where the fluid is fairly stagnant. This accounts for the pressure at the back of the fin being uniform. The one exception to this, in the range studied, occurs when the fin spacing is equal to the fin height. In this case the eddy is almost circular as observed by Knudsen and Katz and completely fills the space between consecutive fins and therefore affects the pressure on the downstream face as well.

Form Drag Coefficients

The form drag for each roughness height and spacing was evaluated by graphically integrating the pressure distributions described in the previous section. A form drag coefficient was then calculated using Equation (5). Figure 10 shows the results for the 1-in. fin. All lines on this

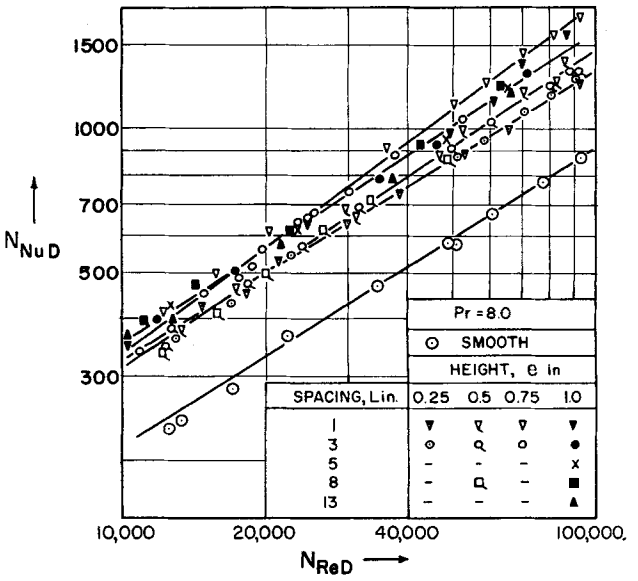

Fig. 14. Effect of Reynolds numbers on heat transfer coefficient for all roughness heights and spacings.

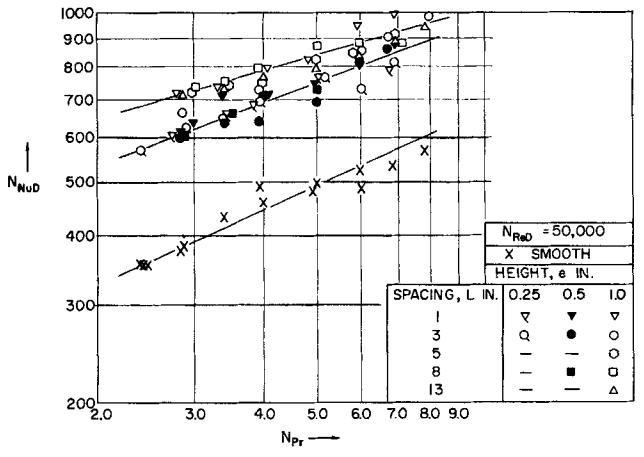

Fig. 15. Effect of Prandtl number on heat transfer coefficient for all roughness heights and spacings.

figure are horizontal and each line represents the arithmetic average of the calculated form drag coefficients for a given spacing. Similar results were obtained using fins of 0.75, 0.50, and 0.25 in. in height.

Figure 11 is a cross-plot of Figure 10 and the graphs (not shown) for the other fin heights. This shows that for all fin heights the form drag approaches zero as the ratio e/L approaches one. Even for spacings twice the fin height, however, the form drag is negligible. For greater spacings the coefficients become large, especially for the high fins.

Skin Friction Coefficients

The net skin-friction contribution to the overall pressure drop was calculated from the measured overall pressure drop and form drag data according to Equation (3). Skin-friction coefficients were calculated using Equation (6). The results for net skin-friction coefficients were somewhat scattered, especially for the large fin spacings where form drag represented a considerable fraction of the total drag. However, the skin-friction coefficient increased as the fins were placed closer together. The contribution of skin friction to the total pressure drop at a Reynolds number of 10^5 can be seen in Figure 12 in which the ratio fs/fT is plotted against the relative fin spacing e/L. For $e/L = 1$ the total pressure drop is owing entirely to a skin-friction effect. The relative contribution of skin friction decreases almost linearly as the spacing increases and appears to pass through a minimum at or below a spacing of $e/L = 1/13$. There appears to be no effect of fin height on the ratio fs/fT.

Heat Transfer Results

The average heat transfer coefficient around the short length of heated tube with the integral test fin was measured for each fin height and fin spacing investigated in the friction studies. In addition, heat transfer coefficients were measured for the test section when the fin was completely machined off; in this case the test section was simply a short length of smooth tube. The average angular temperature variation around the heated section was 5 to 7% of the difference between the mean wall temperature and the water temperature. In some runs the maximum angular variation was 15% and the minimum 1%.

Experimental results on the effect of Reynolds number for the 1-in. fin are shown in Figure 13. It can be seen that the effect of altering the fin spacing was negligible except for a slight decrease in the coefficients for the single fin ($L = \infty$). Figure 14 shows the data for all fin heights and for all spacings other than $L = \infty$. From this figure it is apparent that for all fin heights and spacings investigated, the average heat transfer coefficients around the test element were 70 to 100% greater than the corresponding coefficients for the smooth section.

The heat transfer results for the effect of Prandtl number are shown in Figure 15 for three fin heights and for the smooth test section.

The best line through each set of points in Figure 14 was obtained by the method of least squares. The lines are the result of fitting equations of the form

$$N_{Nu\,D} = a(N_{Re\,D})^n \text{ and } N_{Nu\,D} = b(N_{Pr})^m$$

to the data for each fin height. The best estimates of the values of m and n are shown in Table 2 for each fin height investigated. The Nusselt and Reynolds numbers are based on the empty tube diameter (6.065 in.).

The value of the exponent n for the smooth section was not significantly different from the values of n for the runs at different fin heights. The exponent m, however, was highest for the smooth tube and was significantly lower for the highest fins.

Table 2. Reynolds Number and Prandtl Number Exponents

Height e in.	n	m
Smooth section	0.635	0.45
0.25	0.621	0.37
0.50	0.673	0.37
0.75	0.737	—
1.00	0.650	0.29

DISCUSSION OF RESULTS

Overall friction coefficients were found to be independent of Reynolds number for all roughness configurations and flow rates investigated. This result is in agreement with results for many types of roughened surfaces with extreme roughness protrusions, and has been interpreted as owing to the predominance of inertial over viscous effects in this type of system. The effect of fin height on overall friction coefficient depends on the relative fin spacing e/L. For relative fin spacings in the region of $e/L \sim 1/9$, the effect of fin height is large; for relative fin spacings near $e/L = 1.0$, fin height has very little effect on the overall friction coefficient. At a given fin height, the relative fin spacing has a considerable effect on the overall friction coefficient: the overall coefficient is a maximum for $e/L \sim 1/9$ and a minimum for close spacings where $e/L = 1.0$ to 1.5.

The results for form drag provide new information about the drag forces acting on a roughened surface. Isolated fins have high form drag but the effect of bringing fins closer together is to reduce the form drag on each. For the particular type of fin studied here, decreasing the fin spacing from $L = \infty$ to $L = 10e$ halved the form drag, and spacing the fins two fin heights apart caused the form drag to drop to almost zero. For the case of fin spacing equal to fin height the form drag on each fin was zero. This result is thought to be owing to the unique flow pattern which exists between fins at this spacing.

The difference between overall pressure drop and total form drag must be owing to skin friction. It is apparent that the contribution of skin frictional effects to the total drag is significant over a wide range of relative fin spacings, and that skin friction is solely responsible for all the pressure drop in the systems with $e/L = 1.0$. For the particular case of $e/L = 1.0$, there is the interesting result that the skin friction coefficient is independent of Reynolds number. Now the net skin friction measured in these experiments was owing to the shear stress at the flat surfaces of the tips of the fins and the shear stress at the

base wall between fins. The direction of rotation of the primary eddies between fins implies that at least part of the shear stress at the base wall must act in a direction opposite to that of the shear stress at the fin tips. Secondary eddies in the corners rotate in a direction opposite to that of the primary eddy and cause a shear stress in the same direction as at the fin tips. Hence, the net measured effect will be the algebraic sum of all these effects. The relative contribution of each will depend on the respective areas over which the shear forces act as well as on the magnitudes of these forces.

The heat transfer coefficients obtained are of limited value for predicting heat transfer coefficients in roughened systems heated along their entire length. The results do show that the heat transfer coefficient around a fin (based on the total inside area and taking into account the temperature drop from the base to the tip of the fin) depends only slightly on fin height. The results appear to indicate that heat transfer coefficients are also independent of fin spacing, but this may not in fact be true for large spacings when the heat transfer coefficient along the entire base wall between fins is taken into consideration. The increase in heat transfer coefficient of 75 to 100% over the smooth section value is similar to the increase found in other studies as indicated in the discussion on previous work. The results show that very little improvement in heat transfer coefficient is obtained by increasing the roughness height above about $e/D = 0.04$. For this particular type of finned surface, further increases in the roughness height up to $e/D = 0.165$ can be made with little effect on the heat transfer coefficient; an increased heat transfer rate results mostly from the increase in heat transfer area.

The results for the type of surface investigated in this study do not fit the form of Nunner's equation particularly well. The roughness parameters, fin height and fin spacing, have a much greater effect on overall friction coefficient than on heat transfer coefficient, and there is no evidence to indicate that Prandtl number and overall friction coefficient influence heat transfer in similar ways. However, for the particular case of $e/L = 1$, heat transfer and overall friction coefficients are nearly independent of the roughness parameters in agreement with Nunner's equation.

The results indicate that for a practical heat transfer surface with transverse fins, the fins should be arranged so that e/L is in the range 1.0 to 1.5. This will insure that the overall friction coefficient is a minimum. Provided that the fin height is greater than $e/D = 0.04$, the heat transfer coefficient will be 75 to 100% greater than the equivalent smooth-tube value. A greater heat transfer rate can be obtained by increasing the fin height, the increase in rate being proportional to the increased internal area.

SUMMARY

A study was made of the drag forces which occur when water flows over a surface fitted with protuberances. The effect of protuberances on heat transfer was also measured.

Measurements were made of overall pressure drop and the form drag of an individual protuberance. These data enabled skin friction to be calculated. The effects of Reynolds number and Prandtl number on the average heat transfer coefficient around an integral protuberance were also determined.

The effect of protuberance height and spacing on form drag coefficients was considerable. For each protuberance height, the form drag decreased from a maximum value for an isolated protuberance to zero for a protuberance spacing equal to the protuberance height. The effect of protuberance height on the form drag coefficient decreased as the spacing decreased.

The effect of protuberance height on skin-friction coefficients was very small. At large spacings, the skin-friction coefficients approached the smooth-tube coefficient. The skin-friction coefficients increased as the spacing decreased and reached a constant maximum value, independent of spacing, for spacings closer than the protuberance height.

Heat transfer coefficients were found to increase only slightly with protuberance height. Each protuberance height gave an increase in heat transfer coefficient of about 75 to 100%. An increase in heat transfer rate with increasing protuberance height was therefore owing mostly to an increase in area. The dependence of Nusselt number on Reynolds number was not significantly different from the dependence in smooth tubes. There appeared to be some effect of the fin height on the relation between Nusselt number and Prandtl number; the highest fins gave a somewhat lower exponent on the Prandtl number than was found using the smooth tube.

ACKNOWLEDGMENT

The authors are grateful to the National Science Foundation for supporting this research under grant G 6318. They also acknowledge with gratitude the gift of a section of Lucite pipe by E. I. duPont de Nemours and Company in which visual studies were made and that of a copper billet given by the Wolverine Tube Division of Calumet and Hecla, Incorporated, from which the heat transfer section was made.

NOTATION

A = total inside area of heat transfer section, sq. ft.
A_s = normal area of one side of a roughness element, sq. ft.
a = arbitrary constant
b = arbitrary constant
D = diameter of tube forming the test section, ft.
D_F = total form drag force, lb.$_f$
D'_F = form drag of one roughness element (Equation 4), lb.$_f$
$D_{S,x}$ = skin friction drag force in x direction, lb.$_f$
D_T = total drag force, lb.$_f$
e = height of roughness element, ft.
f_F = form drag coefficient (Equation 5)
f_S = skin-friction coefficient (Equation 6)
f_T = overall friction coefficient (Equation 1)
f_r = overall friction coefficient in a rough tube
f_o = overall friction coefficient in a smooth tube
G = mass rate of flow, lb.$_m$/sec.
g_c = conversion factor, lb.$_m$ ft./lb.$_f$ sec.^{2}
h = isothermal heat transfer coefficient, B.t.u./hr. sq. ft. °F.
L = distance between adjacent roughness elements, ft.
m = arbitrary constant
$N_{Nu\,D}$ = Nusselt number based on diameter of empty test section
$(N_{Nu})_o$ = Nusselt number for smooth tube
$(N_{Nu})_r$ = Nusselt number for rough tube
$N_{Re\,D}$ = Reynolds number based on diameter of empty test section
N_{Pr} = Prandtl number
n = number of roughness elements, arbitrary constant
p = pressure, lb.$_f$/sq. ft.
p_s = reference pressure, lb.$_f$/sq. ft.
p_{yd} = pressure at position y on downstream face of fin
p_{yu} = pressure at position y on upstream face of fin
$\bar{p}_{yd}$ = average pressure on downstream face of fin
Δp_T = overall pressure drop, lb.$_f$/sq. ft.

Δps = pressure drop owing to skin friction, lb.$_f$/sq. ft.
q = rate of heat transfer, B.t.u./hr.
T_b = temperature of water entering heat transfer section, °F.
T_w = average temperature of wall of heat transfer section, °F.
$\overline{U}$ = average velocity of flow, ft./sec.
$\overline{U}_D$ = average velocity of flow based on tube diameter D
$\overline{U}_{D-2e}$ = average velocity of flow based on tube diameter, $D - 2e$, ft.
X = length of measuring section, ft.
x = direction parallel to pipe axis (also used for length of smooth pipe — ft.)
y = direction perpendicular to pipe axis

Greek Letters

$\overline{\tau}$ = average resisting stress at the wall, lb.$_f$/sq. ft.
ρ = water density, lb.$_m$/cu. ft.
ν = kinematic viscosity, sq. ft./sec.
μ_w = viscosity of water at temperature T_w, lb.$_m$/ft. sec.
μ_b = viscosity of water at temperature T_b, lb.$_m$/ft. sec.

LITERATURE CITED

1. Nikuradse, J., *Forsch Arb. Ing. Wesen*, No. 361 (1933).
2. Schlichting, Hermann, *Natl. Advisory Comm. Aeronaut. Tech. Memo* 823 (1936).
3. Stanton, T. E., "Friction," Longmans, Green, (1923).
4. Kemeny, G. A., and J. A. Cyphers, *J. Heat Transfer, Series* C83, 189 (1961).
5. Smith, J. W., and N. J. Epstein, *A.I.Ch.E. Journal*, 3, 242 (1957).
6. Hastrup, R. C., R. H. Sabersky, D. R. Bartz, and M. B. Noel, *Jet Propulsion*, **28**, 259 (1958).
7. Cope, W. F., *Proc. Inst. Mech. Engrs.*, 145 (1941).
8. Dipprey, D. F., Ph.D. thesis, California Inst. of Technol., Pasadena, California (1961).
9. Boelter, L. M. K., G. Young, M. L. Greenfield, V. D. Sanders, and M. Morgan, *Natl. Advisory Comm. Aeronaut. Tech. Note 2517* (1951).
10. Sams, E. W., *Natl. Advisory Comm. Aeronaut.* RM *E52,D17* (1952).
11. Brouillette, E. C., T. R. Mifflin, and J. E. Myers, *Paper No. 57-A-47, Amer. Soc. Mech. Engrs.* (1957).
12. Nunner, Wolfgang, *VDI-Forschungsh. 455*, Series B, **22**, 5 (1956); also Atomic Energy Research Establishment Lib. Trans. 786 (1958).
13. Koch, Rudolf, *VDI-Forschungsh. 469*, Series F, **24** (1958).
14. Knudsen, J. G., and D. L. Katz, *Chem. Eng. Progr.*, **46**, 490 (1950).
15. Wilson, J. T., United Kingdom Atomic Energy Authority *Tech. Memo No. IGR-Tm/w .059* (1956).
16. Harris, M. J., and J. T. Wilson, *J. Brit. Nuclear Energy Conference*, **6**, 330 (1961).
17. Sieder, E. N., and G. E. Tate, *Ind. Eng. Chem.*, **28**, 1429 (1936).
18. Atherton, Arthur, and M. W. Thring, *Trans. Am. Inst. Chem. Engrs.*, 38, 235 (1960).

Manuscript received June 21, 1962; revision received January 17, 1963; paper accepted January 21, 1963.

COMMUNICATIONS TO THE EDITOR

Multicomponent Diffusion in Restricted Systems

E. L. CUSSLER, JR., and E. N. LIGHTFOOT, JR.
University of Wisconsin, Madison, Wisconsin

In an earlier communication (*1*), the authors presented a generalization of the Arnold semi-infinite problem (*2*) to multicomponent systems, starting with the flux equations of Onsager (*3*). The techniques used in that presentation are extended here to the case of unsteady state restricted diffusion. In this case, the system consists of two identical cylindrical compartments, originally filled with uniform multicomponent solutions of slightly different com-